JAST, Vol. 3, No. 3, pp 113–123

JAST
Journal of Aerospace Science and Technology

A Modified Midcourse Guidance Law Based on Generalized Collision Course

S. H. Jalali-Naini[1], S. H. Pourtakdoust[2]

In this paper, analytical solution of the generalized collision course (GCC) is presented considering approximate models for drag and thrust in the presence of gravity. The GCC is near optimal for a considerable flight time toward the end. Therefore, guidance laws based on GCC only need modification for the first stage of flight. The proposed guidance law is a modification of midcourse strategies based on the GCC and its implementation issues. A recursive relation for estimation of time-to-go for the GCC is presented in order to reduce the onboard computational burden. Two other recursive relations for time-to-go are obtained for optimal guidance laws. The relations can be used for both midcourse and terminal applications. For an aerodynamically controlled interceptor, the guidance law produces the commanded acceleration in the direction normal to its velocity vector or approximately normal to its body axis. Simulation results show that the presented strategy is superior to the midcourse guidance laws based on GCC for a greater final velocity.

INTRODUCTION

The requirement for better performance in the midcourse phase needs the development of optimal (suboptimal) guidance laws (OGLs) by the consideration of interceptor tangential acceleration and gravity effect. In the indoatmosphere, the minimization of drag, maximization of final speed, or range may be chosen as a desired objective function for the midcourse phase of flight. The open-loop solution [1,2], singular perturbation theory [3,4], neighboring optimal control techniques about open-loop solutions [5,6], and training a neural network have been presented to solve the problem [7-9].

Conventional air-to-air interceptors use proportional navigation (PN) or some of its modifications. A preprogrammed vertical g-bias command during midcourse as a function of flight time is used to conserve energy in the midcourse phase by flying the interceptor at higher altitudes where air drag is reduced. Empirical methods may also be used to avoid the difficulties of the mathematical closed-loop solution. For instance, a trajectory may be produced by a numerical optimization and some waypoints are selected as virtual targets. Then interceptor will be guided to the waypoints via a closed-loop guidance law such as a modified PN, but before reaching a waypoint exactly, it will switch to the next waypoint. The simplest one for a surface-to-air interceptor is a trapezoidal-shape trajectory in the vertical plane with three waypoints. The last waypoint is the real target. The two other waypoints may be selected with a same altitude. In this approach, the interceptor ascends to the first waypoint, then flies in a constant altitude to reach the second waypoint and finally dives toward the target. The distance between the first two waypoints and their altitudes are functions of the target range and altitude. Another alternative is to use a moving waypoint instead of selecting several waypoints as treated in Ref. [10] for vertical plane. The two-dimensional methods using waypoints must be modified for three-dimensional problems.

The open-loop solution to an optimal midcourse guidance allows us to realize the behavior of an interceptor trajectory and state variables. It is observed that the guidance laws based on optimal control theory can improve performance significantly. The interceptor energy must be conserved during the midcourse phase by flying at higher altitudes with thin air density, so that sufficient energy is available for terminal interception of intelligent targets. The results are useful for

1. *Ph.D. Candidate, Dept. of Aerospace Eng., Sharif Univ. of Tech., Tehran, Iran.*
2. *Professor, Dept. of Aerospace Eng., Sharif Univ. of Tech., Tehran, Iran, Email: pourtak@sharif.edu.*

waypoint guidance as well as for the determination of a preprogrammed vertical g-bias. Numerical solutions are also needed to know how much the available methods, such as PN with vertical g-bias, waypoint guidance, singular perturbation, etc. are close to the optimal solutions.

Singular perturbation theory aids in splitting the optimal guidance problem into a series of low-order subproblems that may be sequentially solved and later combined to obtain an approximate real-time solution to the full-order problem. Cheng and Gupta [3] used singular perturbation theory to develop a midcourse guidance law which minimizes the flight time. They applied singular perturbation theory and engineering approximations to completely eliminate the need for solving two-point boundary value problems (TPBVPs). In the study by Menon and Briggs [4], the cost function minimizes flight time and the specific energy at the final time. The singular perturbation approach in these studies is formulated so that the slow dynamics govern the behavior of cross range, flight path angle and specific energy. Medium dynamics govern the behavior of altitude and fast dynamics are utilized for variations of the pitch and yaw angles.

In 1989, Katzir et al. [5] formulated near-optimal guidance for real-time applications. It is based on a neighboring optimal control concept where a complementary control is added to the precalculated nominal control, but it can fail at some distances from the original TPBVP solution. Another work that makes use of this method was presented by Kumar et al. [6].

Including the thrust and drag effects in the governing equations in the presence of gravitational acceleration and autopilot dynamics is of high interest. The basic ideas for three-dimensional terminal and midcourse atmospheric strategies have been introduced in Refs. [11,12], but the methods lack some implementing issues such as estimating the time-to-go. Therefore, a recursive relation for estimating the time-to-go is derived from generalized relation of zero-effort miss. Moreover, midcourse strategies based on generalized collision course (GCC) are modified to produce a larger final velocity using some additional elevation angle with respect to GCC, specially at the first phase of flight.

ZERO-EFFORT MISS FORMULATION

Here, the governing equation of motion for an interceptor as a particle with perfect guidance and control is modeled as [11]

$$\ddot{\mathbf{r}}_m = -c(t)\mathbf{v}_m + \mathbf{u} + \mathbf{g}(t), \tag{1}$$

where $\mathbf{r}_m$, $\mathbf{v}_m$, and $\mathbf{u}$ denote the interceptor position, velocity, and commanded acceleration vectors with respect to an inertial reference frame ($Oxyz$), respectively. The resultant acceleration due to thrust and drag is modeled by the term $-c(t)\mathbf{v}_m$. The problem of modeling is resolved later using an approximate relation of $c(t) \simeq -\dot{v}_m/v_m$. The model implies that the thrust vector is assumed along the velocity vector. The gravitational acceleration,$\mathbf{g}(t)$, is taken as a vectorial function of time. The wind effect can also be included in $\mathbf{g}(t)$ as a vectorial function of time.

By integrating Eq. (1) twice with respect to time, the interceptor position is obtained as

$$\mathbf{r}_m(t) = \mathbf{r}_{m_0} + \beta_1(t,t_0)\mathbf{v}_{m_0} + \int_{t_0}^{t} \beta_1(t,\xi)[\mathbf{u}(\xi) + \mathbf{g}(\xi)]d\xi, \tag{2}$$

where

$$\beta_1(t,t_0) = \int_{t_0}^{t} e^{-\int_{t_0}^{\eta} c(\xi)d\xi} d\eta. \tag{3}$$

The final position of the interceptor in terms of current states is then given by

$$\mathbf{r}_m(t_f) = \mathbf{r}_m + \beta_1(t_f,t)\mathbf{v}_m + \int_{t}^{t_f} \beta_1(t_f,\xi)[\mathbf{u}(\xi) + \mathbf{g}(\xi)]d\xi. \tag{4}$$

It is desired to reach the final position $\mathbf{r}^*_{m_f}$. The zero-effort miss, **ZEM**(t), is the distance that the interceptor would miss its target position if the interceptor made no corrective maneuver after the time t, that is,

$$\mathbf{ZEM}(t) = \mathbf{r}^*_{m_f} - \mathbf{r}_m(t_f), \quad \mathbf{u}(\xi) = \mathbf{0} \text{ for } t < \xi \leq t_f. \tag{5}$$

To intercept a moving target, the desired interceptor final position must be the target final position, i.e., $\mathbf{r}^*_{m_f} = \mathbf{r}_t(t_f)$. The subscripts "$m$" and "$t$" represent interceptor and target, respectively. Assuming the interceptor autopilot to be perfect, the zero-effort miss is found to be [11]

$$\mathbf{ZEM} = \mathbf{r}^*_{m_f} - \mathbf{r}_m - \mathbf{v}_m\beta_1(t_f,t) - \int_{t}^{t_f} \beta_1(t_f,\xi)\mathbf{g}(\xi)d\xi. \tag{6}$$

MIDCOURSE GUIDANCE BASED ON GCC

The generalized collision course is an interceptor trajectory that would cause a perfect intercept if the commanded acceleration were set to zero. The interceptor velocity that causes the ZEM to become zero is denoted by $\mathbf{v}_{m_{cc}}$; therefore, [12]

$$\mathbf{v}_{m_{cc}} = \frac{\mathbf{r}^*_{m_f} - \mathbf{r}_m - \int_t^{t_f} \beta_1(t_f,\xi)\mathbf{g}(\xi)d\xi}{\beta_1(t_f,t)}. \tag{7}$$

Hence, it is concluded that:

$$\mathbf{v}_{m_{cc}} - \mathbf{v}_m = \mathbf{ZEM}/\beta_1(t_f,t). \tag{8}$$

The objective of guidance laws based on GCC can be written as:

$$\mathbf{v}_{m_{cc}} - \mathbf{v}_m = \mathbf{0}, \tag{9a}$$

$$\mathbf{v}_{m_{cc}} \times \mathbf{v}_m = \mathbf{0}. \tag{9b}$$

The commanded acceleration is considered proportional to the preceding relations in the appropriate direction, that is,

$$\mathbf{u} = K_v(\mathbf{v}_{m_{cc}} - \mathbf{v}_m), \tag{10a}$$

$$\mathbf{u}_n = K_\phi(\mathbf{e}_m \times \mathbf{e}_{m_{cc}}) \times \mathbf{e}_m, \tag{10b}$$

where $\mathbf{u}_n$ is the commanded acceleration in the direction normal to the interceptor velocity; $\mathbf{e}_m$ and $\mathbf{e}_{m_{cc}}$ are the unit vectors of $\mathbf{v}_m$ and $\mathbf{v}_{m_{cc}}$, respectively. Note that the commanded accelerations in Eqs. (10a,b) are in the direction of ZEM (or opposite to it) and normal to the interceptor velocity, respectively.

The explicit guidance is in the form of $\mathbf{u} = \Lambda\,\mathbf{ZEM}$ where Λ is the guidance gain. The commanded acceleration is also usually expressed as $\mathbf{u} = (N'/t_g^2)\mathbf{ZEM}$ where t_g is the time-to-go until intercept and N' is the effective navigation ratio in comparison with True PN. Comparing Eq. (10a) with Eq. (8) yields

$$\mathbf{u} = \Lambda\beta_1(t_f,t)(\mathbf{v}_{m_{cc}} - \mathbf{v}_m). \tag{11}$$

Thus K_v may be chosen as

$$K_v = \Lambda\beta_1(t_f,t). \tag{12}$$

By the assumption $v_m = v_{m_{cc}}$, we have

$$\mathbf{u} = \Lambda\beta_1(t_f,t)v_m(\mathbf{e}_{m_{cc}} - \mathbf{e}_m). \tag{13}$$

In the case of small heading error, the term $(\mathbf{e}_{m_{cc}} - \mathbf{e}_m)$ becomes normal to interceptor velocity. One way to obtain K_ϕ is to equate Eqs. (10b) and (13), and obtain

$$K_\phi = \Lambda\beta_1(t_f,t)v_m\phi/\sin\phi, \tag{14}$$

where ϕ is the angle between $\mathbf{v}_m$ and $\mathbf{v}_{m_{cc}}$ [12].

VELOCITY PROFILE PREDICTION

The presented guidance strategies need the prediction of $c(t)$ or interceptor velocity profile. Here, it is assumed that the thrust acceleration is in the direction of the interceptor velocity. This assumption is reasonable for the midcourse phase in the endoatmosphere when the acceleration requirement is low as it is in many applications. A relation for $c(t)$ may be fitted for a given interceptor in terms of target position and velocity by using simulation data. Coefficients of this relation may be updated in flight using a look-up table. Approximate predictions may also be used for this matter. An approximate relation of $c(t) \simeq -\dot{v}_m/v_m$ may be utilized, so we have

$$\int_t^\eta c(\xi)d\xi \simeq -\int_{v_m(t)}^{v_m(\eta)} \frac{dv_m}{v_m} = \ln\frac{v_m(t)}{v_m(\eta)}. \tag{15}$$

Therefore,

$$\beta_1(t_f,t) = \int_t^{t_f} e^{-\int_t^\eta c(\xi)d\xi}d\eta \simeq \frac{1}{v_m(t)}\int_t^{t_f} v_m(\eta)d\eta. \tag{16}$$

On the other hand, the interceptor tangential acceleration $a_v = dv_m/dt$ integrates into:

$$v_m(\eta) = v_m(t) + \int_t^\eta a_v(\xi)d\xi. \tag{17}$$

Substituting the preceding relation into Eq. (16) yields:

$$\beta_1(t_f,t) \simeq t_g + \frac{1}{v_m(t)}\int_t^{t_f}\int_t^\eta a_v(\xi)d\xi d\eta. \tag{18}$$

Simplifying the double integral to a single one results in:

$$\beta_1(t_f,t) \simeq t_g + \frac{\int_t^{t_f}(t_f-\xi)a_v(\xi)d\xi}{v_m(t)} = \frac{\int_t^{t_f} v_m(\eta)d\eta}{v_m(t)}. \tag{19}$$

In order to simplify the above equation, consider the following averaging definitions:

$$\tilde{a}_v = \frac{\int_t^{t_f}(t_f-\xi)a_v(\xi)d\xi}{t_g^2}, \tag{20}$$

$$\bar{v}_m = \frac{\int_t^{t_f} v_m(\xi)d\xi}{t_g} = v_m + \tilde{a}_v t_g, \tag{21}$$

where $\bar{v}_m$ is the average velocity between the current and final times and $\tilde{a}_v$ is the time-to-go weighted average of the tangential acceleration. One can now rewrite Eq. (19) as

$$\beta_1(t_f,t) \simeq t_g + \frac{\tilde{a}_v}{v_m}t_g^2\,, \qquad \beta_1(t_f,t) \simeq \frac{\bar{v}_m}{v_m}t_g. \tag{22}$$

When the approximate relation $c(t) \simeq -\dot{v}_m/v_m$ is utilized, the component of gravity along the interceptor velocity must be included in $c(t)$. Therefore, Eq. (1) is converted into

$$\ddot{\mathbf{r}} = -c(t)\mathbf{v}_m + \mathbf{u} + \mathbf{g}_n, \tag{23}$$

where $\mathbf{g}_n$ denotes the gravitational acceleration normal to interceptor velocity. In this formulation, $\mathbf{g}$ must be replaced by $\mathbf{g}_n$ in ZEM and time-to-go relations. The commanded acceleration is taken approximately normal to interceptor velocity in aerodynamically controlled interceptors. The tangential acceleration a_v is

the resultant of nongravitational acceleration (a_{ng}^v) and gravitational acceleration ($-g\sin\gamma$) in the direction along interceptor velocity. For a better estimation of $\beta_1(t_f,t)$, the gravitational and nongravitational accelerations along the interceptor velocity may be modeled separately. We can thus write

$$\tilde{a}_v t_g^2 = \left[\int_t^{t_f}(t_f-\xi)a_{ng}^v(\xi)d\xi - g\int_t^{t_f}(t_f-\xi)\sin\gamma(\xi)d\xi\right], \tag{24}$$

where γ is the interceptor flight-path angle. The estimation of γ is also needed. Using Eqs. (21-23) results in [12]

$$\begin{aligned}\mathbf{ZEM} &= \mathbf{r}_{m_f}^* - \mathbf{r}_m - \mathbf{v}_m t_g - \tilde{a}_v t_g^2 \mathbf{e}_m - \int_t^{t_f}\beta_1(t_f,\xi)\mathbf{g}_n(\xi)d\xi \\ &= \mathbf{r}_{m_f}^* - \mathbf{r}_m - \bar{v}_m t_g \mathbf{e}_m - \int_t^{t_f}\beta_1(t_f,\xi)\mathbf{g}_n(\xi)d\xi,\end{aligned} \tag{25}$$

where $\mathbf{g}_n(t)=\mathbf{g}+g\mathbf{e}_m\sin\gamma$. A simplified relation for β_1 may be used in the preceding relation, e.g., β_1 without gravity effect.

Multi-Constant Profile

Consider the tangential acceleration of an interceptor can be modeled as a multi-constant profile, that is,

$$\dot{v}_m = a_i \quad \text{for} \quad t_{i-1} \le t < t_i\ , \quad i=1,2,...,N \tag{26}$$

where a_i's are constants and $t_N = t_f$. Therefore, for $t_{j-1} \le t < t_j$, we have

$$\begin{aligned}\int_t^{t_f}(t_f-\xi)a_v(\xi)d\xi &= \int_t^{t_j}(t_f-\xi)a_j d\xi \\ &\quad + \sum_{i=j}^{N-1}\int_{t_i}^{t_{i+1}}(t_f-t)a_{i+1}dt,\end{aligned} \tag{27}$$

which integrates into

$$\begin{aligned}\int_t^{t_f}(t_f-\xi)a_v(\xi)d\xi &= \frac{1}{2}[t_g^2-(t_f-t_j)^2]a_j \\ &\quad + \frac{1}{2}\sum_{i=j}^{N-1}a_{i+1}[(t_f-t_i)^2-(t_f-t_{i+1})^2].\end{aligned} \tag{28}$$

Boost-Sustain-Coast

Consider an interceptor with a booster and sustainer motor in a way that the interceptor velocity is kept constant in the sustained phase. After the burnout of the sustainer motor at $t=t_{p_2}$, a constant tangential deceleration (a_d) will be used, that is,

$$\dot{v}_m = \begin{cases} a_x & \text{for } t \le t_p \\ 0 & \text{for } t_p < t \le t_{p_2} \\ a_d & \text{for } t > t_{p_2} \end{cases} \tag{29}$$

The relation for $\beta_1(t_f,t)$ can be obtained for $t \le t_p$ as

$$\beta_1(t_f,t) \simeq t_{go} + \frac{a_x}{2v_m}[t_{go}^2-(t_f-t_p)^2] + \frac{a_d}{2v_m}(t_f-t_{p_2})^2 \tag{30}$$

or

$$\begin{aligned}\beta_1(t_f,t) &\simeq t_{go} + \frac{a_x}{2v_m}t_{pg}(2t_{go}-t_{pg}) \\ &\quad + \frac{a_d}{2v_m}(t_{go}-t_{pg}-T_{\text{sus}})^2,\end{aligned} \tag{31}$$

where $T_{\text{sus}} = t_{p_2} - t_p$ is the duration of the sustained phase. For $t_p < t \le t_{p_2}$ we have

$$\beta_1(t_f,t) \simeq t_{go} + \frac{a_d}{2v_m}(t_f-t_{p_2})^2 = t_{go} + \frac{a_d}{2v_m}(t_{go}-t_{pg_2})^2, \tag{32}$$

where $t_{pg_2} = t_{p_2} - t$ is the time to the burnout of the sustainer motor. For $t > t_{p_2}$ we have $\beta_1(t_f,t) = t_{go} + 0.5\,a_d\,t_{go}^2/v_m$.

In the case in which the tangential acceleration is modeled in the form of

$$\dot{v}_m = \begin{cases} a_x & \text{for } t \le t_p \\ 0 & \text{for } t_p < t \le t_{p_2} \\ -c_3 v_m & \text{for } t > t_{p_2} \end{cases} \tag{33}$$

the relation for $\beta_1(t_f,t)$ can be obtained for constant $c_3 > 0$ and $t \le t_p$ as:

$$\begin{aligned}\beta_1(t_f,t) &\simeq t_{pg} + \frac{a_x t_{pg}^2}{2v_m} + T_{\text{sus}}\left[1+\frac{a_x t_{pg}}{v_m}\right] \\ &\quad + \frac{1}{c_3}\left[1+\frac{a_x t_{pg}}{v_m}\right]\left[1-e^{-c_3(t_{go}-t_{pg}-T_{\text{sus}})}\right].\end{aligned} \tag{34}$$

For $t_p < t \le t_{p_2}$ we obtain:

$$\beta_1(t_f,t) \simeq t_{pg_2} + \frac{1}{c_3}\left[1-e^{-c_3(t_{go}-t_{pg_2})}\right]. \tag{35}$$

For $t > t_{p_2}$ we have $\beta_1(t_f,t) \simeq (1-e^{-c_3 t_{go}})/c_3$.

MODIFIED GUIDANCE FORMULATION

Simulation results show that the midcourse guidance laws based on GCC cannot produce maximum final velocity. On the other hand, the GCC will be near optimal for a considerable flight time toward the end,

if an appropriate modification is utilized for the first phase of flight in order to achieve a larger final velocity [14]. Here, these types of guidance laws are modified by defining a desired interceptor velocity obtained by rotation of $\mathbf{v}_{m_{cc}}$ in the vertical plane through the angle of γ_e. In other words, an additional flight path angle with respect to the GCC is imposed in the vertical plane. First, the projection of $\mathbf{v}_{m_{cc}}$ in the horizontal plane is obtained as follows:

$$\mathbf{v}_{m_{cc_{xy}}} = \mathbf{v}_{m_{cc}} - (\mathbf{v}_{m_{cc}} \cdot \mathbf{e}_k)\mathbf{e}_k, \tag{36}$$

where $\mathbf{e}_k$ is the unit vector of the vertical direction z. The elevation angle of $\mathbf{v}_{m_{cc}}$ is denoted by γ_{cc}, that is,

$$\tan\gamma_{cc} = \frac{v_{m_{cc_z}}}{\sqrt{v^2_{m_{cc_x}} + v^2_{m_{cc_y}}}}, \tag{37}$$

where the subscripts x, y, and z represent the components along x, y, and z axes, respectively. Therefore, the desired interceptor velocity direction is:

$$\mathbf{e}^*_m = \mathbf{e}_{m_{xy}}\cos(\gamma_{cc} + \gamma_e) + \mathbf{e}_k \sin(\gamma_{cc} + \gamma_e), \tag{38}$$

where $\mathbf{e}_{m_{xy}}$ is the unit vector of $\mathbf{v}_{m_{cc_{xy}}}$. The commanded acceleration in the direction normal to interceptor velocity is then calculated by:

$$\mathbf{u}_n = \Lambda\beta_1(t_f, t)v_m(\mathbf{e}_m \times \mathbf{e}^*_m) \times \mathbf{e}_m. \tag{39}$$

The relation for γ_e may be chosen as

$$\gamma_e(t) = (\gamma_L - \gamma_{cc_0})\left(\frac{t_g - T_{TG}}{t + t_g}\right) \qquad \text{for } t_g > T_{TG} \tag{40}$$

where γ_L is the launch angle, $\gamma_{cc_0} = \gamma_{cc}(t = 0)$, and T_{TG} is the GCC duration or terminal phase duration. For $t_g \le T_{TG}$ we apply $\gamma_e = 0$ or PN guidance law. Also, γ_e may be determined in a way that the initial acceleration command becomes zero. In other words, the launch angle and guidance law must be compatible.

ESTIMATION OF TIME-TO-GO

The simplest relation for estimating the time-to-go is $t_g = -r/v_c$, where $v_c = -\dot{r}$ is the closing velocity. This estimation is exact for the collision course for which the interceptor and target velocity are constants. In a better approximation, v_c may be replaced by the average closing velocity between the current and final times denoted by $\bar{v}_c$, but this average quantity is a function of time-to-go. The estimation of time-to-go may lead to a transcendental algebraic equation or in special cases, it may be modeled by a high-order polynomial. Solving this equation and also making a logical decision to select an appropriate root is usually a considerable computational burden and not appropriate for practical implementation. In case the value of time-to-go is available for the past 0.01 sec, it is reasonable to compute the average closing velocity using the result of the posterior step, i.e.,

$$t_g(n+1) = r(n+1)/\bar{v}_c(t_g(n)), \tag{41}$$

where n denotes discrete time index. It should be noted that the frequency of computing the commanded acceleration is, for example, 100 Hertz, so time-to-go is calculated for every 0.01 sec. To do this, a second-order polynomial of t_g may be utilized [14], that is,

$$At_g^2 + v_c t_g - t = 0, \tag{42}$$

where A is the average relative acceleration along the line-of-sight (LOS) between interceptor and its target. Therefore [14],

$$t_g = r/(v_c + At_g). \tag{43}$$

Solving Eq. (42) for $1/t_g$ yields the Rigg's equation for the estimation of time-to-go. The correct root is [13,14]

$$t_g = \frac{2r}{v_c + \sqrt{v_c^2 + 4Ar}}. \tag{44}$$

The preceding relation implies that the average closing velocity is:

$$\bar{v}_c = (v_c + \sqrt{v_c^2 + 4Ar})/2. \tag{45}$$

To compute A, the estimation of time-to-go from the previous step is utilized. The above mentioned formulation is employed in the guidance laws based on zero-effort miss as discussed in the second approach of this section.

There are several conceptual approaches to estimate the time-to-go which lead, in general, to a transcendental algebraic equation for t_g. To explain the procedure for developing a recursive relation, first assume a polynomial of order six for t_g as follows:

$$c_6t_g^6 + c_5t_g^5 + c_4t_g^4 + c_3t_g^3 + c_2t_g^2 + c_1t_g + c_0 = 0. \tag{46}$$

Therefore,

$$c_6t_g^4 + c_5t_g^3 + c_4t_g^2 + c_3t_g + c_2]t_g^2 + c_1t_g + c_0 = 0 \tag{47}$$

or

$$A(t_g)t_g^2 + c_1t_g + c_0 = 0. \tag{48}$$

Any transcendental equation is converted into the preceding form, so $A(t_g)$ has, in general, a transcendental form. Dividing Eq. (48) by t_g^2 yields:

$$c_0\left(\frac{1}{t_g}\right)^2 + c_1\left(\frac{1}{t_g}\right) + A = 0. \tag{49}$$

Solving the quadratic equation (49) results in

$$t_g = \frac{2c_0}{-c_1 \pm \sqrt{c_1^2 - 4c_0A}}. \tag{50}$$

The values for c_0 and c_1, and the relation of $A(t_g)$ depend on the selected approach for estimating t_g.

First approach:
The ZEM and $\mathbf{v}_{m_{cc}}$ depend on the value of the final time t_f or the time-to-go until intercept. There could be several methods for estimating t_g. Here, the time-to-go until intercept is calculated for the GCC and denoted by t_g^*. To calculate $\mathbf{v}_{m_{cc}}$ and t_g^*, we have one vectorial relation for ZEM (3 scalar equations) which is set to zero, that is,

$$\mathbf{r}_t(t_f^*) - \mathbf{r}_m - \mathbf{v}_{m_{cc}}\beta_1(t_f^*,t) - \int_t^{t_f^*} \beta_1(t_f^*,\xi)\mathbf{g}(\xi)d\xi = \mathbf{0}. \tag{51}$$

By the assumption $|\mathbf{v}_{m_{cc}}| = |\mathbf{v}_m|$, the number of equations and unknown variables becomes equal. The solution may be found numerically [12]. The target final position may be modeled in the form of

$$\mathbf{r}_t(t_f) = \mathbf{r}_t + \mathbf{v}_t t_g, \tag{52}$$

where $\mathbf{r}_t$ and $\mathbf{v}_t$ are the target position and velocity in $Oxyz$ inertial reference, respectively. With the definition of the relative position, $\mathbf{r} = \mathbf{r}_t - \mathbf{r}_m$, Eq. (51) is rewritten as:

$$\mathbf{ZEM} = \mathbf{r} + \mathbf{v}_t t_g^* - \mathbf{v}_{m_{cc}}\beta_1(t_f^*,t) - \int_t^{t_f^*} \beta_1(t_f^*,\xi)\mathbf{g}(\xi)d\xi = \mathbf{0}. \tag{53}$$

Using the assumption $|\mathbf{v}_{m_{cc}}| = |\mathbf{v}_m|$, we have

$$\left|\mathbf{r} + \mathbf{v}_t t_g^* - \int_t^{t_f^*} \beta_1(t_f^*,\xi)\mathbf{g}(\xi)d\xi\right| = v_m\beta_1(t_f^*,t). \tag{54}$$

Therefore,

$$r^2 + v_t^2 t_g^{*2} - v_m^2\beta_1^2(t_f^*,t) + 2\mathbf{r}\cdot\mathbf{v}_t t_g^* - 2(\mathbf{r}+\mathbf{v}_t t_g^*)\cdot \int_t^{t_f^*} \beta_1(t_f^*,\xi)\mathbf{g}(\xi)d\xi + \left[\int_t^{t_f^*} \beta_1(t_f^*,\xi)\mathbf{g}(\xi)d\xi\right]^2 = 0. \tag{55}$$

The solution of the preceding relation gives t_f^* or t_g^*. Using the mentioned procedure results in:

$$t_g^* = \frac{r}{-\mathbf{v}_t\cdot\mathbf{e}_r + \sqrt{(\mathbf{v}_t\cdot\mathbf{e}_r)^2 - A^*}}, \tag{56}$$

where

$$A^* = v_t^2 - \frac{\beta_1^2(t_f^*,t)}{t_g^{*2}}v_m^2 + \frac{1}{t_g^{*2}}\left[\int_t^{t_f^*} \beta_1(t_f^*,\xi)\mathbf{g}(\xi)d\xi\right]^2 + \frac{2}{t_g^{*2}}(\mathbf{r}+\mathbf{v}_t t_g^*)\cdot\int_t^{t_f^*} \beta_1(t_f^*,\xi)g(\xi)d\xi, \tag{57}$$

and $\mathbf{e}_r = \mathbf{r}/r$ is the unit vector along the interceptor-target LOS. In this case, $c_0 = r^2$ and $c_1 = 2(\mathbf{r}\cdot\mathbf{v}_t)$. To calculate A^* we use t_g^* from the previous step.

Using Eq. (22) for $\beta_1(t_f,t)$ and neglecting the component of gravity normal to the interceptor velocity, Eq. (57) simplifies to

$$A^* = v_t^2 - \bar{v}_m^2. \tag{58}$$

Hence,

$$t_g^* = \frac{r}{-\mathbf{v}_t\cdot\mathbf{e}_r + \sqrt{\bar{v}_m^2 - v_{t_{PLOS}}^2}}, \tag{59}$$

where $v_{t_{PLOS}}$ is the component of the target velocity perpendicular to LOS.

In the case in which the interceptor velocity is constant, t_g^* is given by [12]

$$t_g^* = \frac{r}{-\mathbf{v}_t\cdot\mathbf{e}_r + \sqrt{v_m^2 - v_{t_{PLOS}}^2}}. \tag{60}$$

Therefore, Eq. (59) can be considered as a generalized form by replacing $\bar{v}_m$ for v_m. Discussion on the existence of t_g for Eq. (59) is simple. In practice, the interceptor velocity is greater than the target velocity, so $\bar{v}_m \geq |v_{t_{PLOS}}|$ and we have a real solution. For approaching targets ($\mathbf{v}_t\cdot\mathbf{e}_r < 0$), t_g is positive. For a receding target, we obtain $\bar{v}_m > \sqrt{2}\,|v_{t_{PLOS}}|$. Hence, when $\bar{v}_m > \sqrt{2}|v_{t_{PLOS}}|$, Eq. (59) gives a positive value for t_g.

Second approach:
A very common approach in the literature to estimate t_g is to use the following equation when the relation $\mathbf{u} = \Lambda\,\mathbf{ZEM}$ is utilized:

$$\mathbf{ZEM}\cdot\mathbf{e}_r = 0. \tag{61}$$

Therefore, the commanded acceleration becomes normal to ZEM, that is,

$$\mathbf{u} = \Lambda\,\mathbf{ZEM}_{\mathrm{PLOS}}, \tag{62}$$

where the subscript "PLOS" represents in the direction perpendicular to LOS. Using Eq. (61) we obtain:

$$\left[\mathbf{r} + \mathbf{v}_t t_g - \mathbf{v}_m\beta_1(t_f,t) - \int_t^{t_f} \beta_1(t_f,\xi)\mathbf{g}(\xi)d\xi\right]\cdot\mathbf{e}_r = 0. \tag{63}$$

By the definition $\beta_1(t_f,t) = t_g + \beta_1'(t_f,t)$, one can obtain:

$$r + \dot{r}t_g - (\mathbf{v}_m\cdot\mathbf{e}_r)\beta_1'(t_f,t) - \left[\int_t^{t_f} \beta_1(t_f,\xi)\mathbf{g}(\xi)d\xi\right]\cdot\mathbf{e}_r = 0. \tag{64}$$

Using Eqs. (22) and (23), Eq. (64) is rewritten as:

$$r+\dot{r}t_g-\left\{\tilde{a}_v\cos\phi_m+\frac{1}{t_g^2}\left[\int_t^{t_f}\beta_1(t_f,\xi)\mathbf{g}_n(\xi)d\xi\right]\cdot\mathbf{e}_r\right\}t_g^2=0, \tag{65}$$

where ϕ_m is the angle between the interceptor velocity and LOS. Using a procedure like treated in Eqs. (48-50) we obtain:

$$t_g=\frac{2r}{v_c+\sqrt{v_c^2+4r\tilde{a}_v\cos\phi_m+\frac{4}{t_g^2}\left[\int_t^{t_f}\beta_1(t_f,\xi)\mathbf{g}_n(\xi)d\xi\right]\cdot\mathbf{e}_r}}. \tag{66}$$

Without gravity effect, Eq. (66) simplifies to

$$t_g=\frac{2r}{v_c+\sqrt{v_c^2+4r\tilde{a}_v\cos\phi_m}}. \tag{67}$$

The preceding relation is comparable with those mentioned in the literature [13,14].

Third approach:
Here, t_g is calculated in a way that $|\mathbf{ZEM}|$ is minimized. In other words, $\partial|\mathbf{ZEM}|/\partial t_g = 0$. For simplicity, consider the following relation for ZEM as a special case:

$$\mathbf{ZEM}=\mathbf{r}+\mathbf{v}t_g-\frac{1}{2}a_v t_g^2\mathbf{e}_m, \tag{68}$$

where $\mathbf{v}=\mathbf{v}_t-\mathbf{v}_m$ is the relative velocity and the tangential acceleration a_v is, here, assumed constant. We can thus write

$$\mathrm{ZEM}^2=\frac{1}{4}a_v^2t_g^4-a_v(\mathbf{v}\cdot\mathbf{e}_m)t_g^3+(v^2-ra_v\cos\phi_m)t_g^2+2r\dot{r}t_g+r^2. \tag{69}$$

Using the relation $\partial|\mathbf{ZEM}|^2/\partial t_g=0$ yields:

$$a_v^2t_g^3-3a_v(\mathbf{v}\cdot\mathbf{e}_m)t_g^2+2(v^2-ra_v\cos\phi_m)t_g+2r\dot{r}=0. \tag{70}$$

The preceding cubic equation may be solved analytically, but for the general case, the procedure used in Eqs. (48-50) is suggested.

The recursive relations developed in this section need an initial value for the time-to-go, i.e., t_f which is computed at the launch site. In the launch site, the original transcendental algebraic equation may be solved to obtain t_f.

Special Case: short-range applications
The ZEM relation for a target with constant acceleration $\mathbf{a}_t$ and without gravity effect is given by

$$\mathbf{ZEM}=\mathbf{r}+\mathbf{v}t_g+\frac{1}{2}\mathbf{a}_t t_g^2-\tilde{a}_v t_g^2\mathbf{e}_m. \tag{71}$$

Using Eq. (61) for the estimation of t_g yields

$$r+\dot{r}t_g-(\tilde{a}_v\cos\phi_m-\frac{1}{2}\mathbf{a}_t\cdot\mathbf{e}_r)t_g^2=0. \tag{72}$$

Solving the preceding quadratic equation for $1/t_g$ results in

$$t_g=\frac{2r}{v_c+\sqrt{v_c^2+2r(2\tilde{a}_v\cos\phi_m-a_{t_{\mathrm{LOS}}})}}, \tag{73}$$

where $a_{t_{\mathrm{LOS}}}=\mathbf{a}_t\cdot\mathbf{e}_r$. The relation for $\mathbf{ZEM}_{\mathrm{PLOS}}$ is then given by

$$\mathbf{ZEM}_{\mathrm{PLOS}}=(\boldsymbol{\Omega}\times\mathbf{r})t_g-\tilde{a}_v(\mathbf{e}_m-\cos\phi_m\mathbf{e}_r)t_g^2+\frac{1}{2}\mathbf{a}_{t_{\mathrm{PLOS}}}t_g^2, \tag{74}$$

where $\boldsymbol{\Omega}=(\mathbf{r}\times\mathbf{v})/r^2$ is the LOS turning rate, $\cos\phi_m=\mathbf{e}_m\cdot\mathbf{e}_r$, and

$$\mathbf{a}_{t_{\mathrm{PLOS}}}=\mathbf{a}_t-(\mathbf{a}_t\cdot\mathbf{e}_r)\mathbf{e}_r. \tag{75}$$

Since $\tilde{a}_v$ generally depends on time-to-go, t_g cannot be omitted from the relation of acceleration command.

In the case in which the tangential acceleration is constant, we have $\tilde{a}_v=\frac{1}{2}a_v$. Therefore, using Eqs. (62), (73), and (74) we arrive at

$$\mathbf{u}=\tfrac{N'}{2}[v_c+\sqrt{v_c^2+2r(a_v\cos\phi_m-a_{t_{\mathrm{LOS}}})}\,](\boldsymbol{\Omega}\times\mathbf{e}_r)-\tfrac{N'}{2}a_v(\mathbf{e}_m-\cos\phi_m\mathbf{e}_r)+\tfrac{N'}{2}\mathbf{a}_{t_{\mathrm{PLOS}}} \tag{76}$$

The preceding relation is a modified Augmented PN for an interceptor with constant tangential acceleration. In this case, $a_v=a_x\cos\alpha$ where a_x is the interceptor axial acceleration and α is the angle of attack. For implementation, Eq. (76) may be changed in the following form:

$$\mathbf{u}=\tfrac{N'}{2}[v_c+\sqrt{v_c^2+2r(a_x\cos L-a_{t_{\mathrm{LOS}}})}\,](\boldsymbol{\Omega}\times\mathbf{e}_r)-\tfrac{N'}{2}a_x(\mathbf{e}_x-\cos L\ \mathbf{e}_r)+\tfrac{N'}{2}\mathbf{a}_{t_{\mathrm{PLOS}}}. \tag{77}$$

where $\mathbf{e}_x$ is the unit vector along body axis and L is the look angle, i.e., the angle between LOS and body axis ($\cos L=\mathbf{e}_x\cdot\mathbf{e}_r$).

SIMULATION RESULTS

To compare several PN strategies with/without vertical g-bias and the proposed guidance laws, computer simulation is utilized. The interceptor and target are taken as particles with perfect dynamics. The thrust

acceleration is assumed in the direction of velocity and the commanded acceleration is applied in the direction normal to velocity. The governing equation of motion is

$$\mathbf{a}_m = \frac{T-D}{m(t)}\mathbf{e}_m + \mathbf{u}_n + \mathbf{g}, \tag{78}$$

where T and D are thrust and drag forces, respectively; $m(t)$ is the interceptor mass, and $\mathbf{g}$ is assumed constant. Also,

$$T = gI_{sp}\dot{m}, \quad D = \frac{1}{2}\rho v_m^2 S_{\text{ref}} C_D, \quad S_{\text{ref}} = \pi d^2/4, \tag{79}$$

where I_{sp} is specific impulse, $\dot{m}$ is mass flow rate, ρ is air density, and d is the interceptor diameter. The air density is calculated using the 1962 International Standard Atmosphere ISO 2533. The drag polar equation $C_D = C_{D_0} + KC_L^2$ is utilized where

$$C_{D_0}(M) = \begin{cases} 0.3 & \text{for } M \le 0.8 \\ \frac{-0.36+0.8M-0.1M^2}{\sqrt{M^2-1}} & \text{for } M \ge 1.2 \end{cases} \tag{80}$$

$$K(M) = \begin{cases} 0.025 & \text{for } M \le 0.8 \\ \frac{5.8M^2-16M+47}{1000} & \text{for } M \ge 1.2 \end{cases} \tag{81}$$

and C_L is lift coefficient and M is Mach number. The values of C_{D_0} and K for the transonic region are calculated by the linear interpolation of the data at $M = 0.8$ and 1.2. The launch mass is 650 kg and $I_{sp} = 270$ sec. The mass flow rate for boosting and sustain phases are $\dot{m}_1 = -32$ kg/s for 6 seconds and $\dot{m}_2 = -5.7$ kg/s for 19 seconds, respectively. It should be noted that the interceptor is modeled as a point mass, but the induced drag is calculated using drag polar equation. Since the autopilot/airframe is assumed perfect and u_n is the lift acceleration, so $C_L = mu_n/(\frac{1}{2}\rho v_m^2 S_{\text{ref}})$ is substituted into the drag polar equation. The interceptor initial position is $[0\ 0\ 1]^T$ m; the initial velocity is 27 m/s; and the minimum and maximum launcher elevation angles are 14 and 70 (deg), respectively. The guidance turn-on time is 2 seconds.

To the authors' knowledge, there are two relations for PN with vertical g-bias in the open literature as follows:

$$u = N'v_c\Omega + g_{\text{PLOS}}, \tag{82}$$

$$u = N'v_c\Omega + (N'/2)g_{\text{PLOS}}. \tag{83}$$

The first relation comes from the classical concept that any acceleration normal to LOS must be compensated in the acceleration command so that the net relative acceleration normal to LOS becomes equal to $N'v_c\Omega$. The latter comes from the optimal control formulation when Eq. (61) is utilized for estimation of t_g. However, it seems another g-bias is used for the midcourse phase, but not published yet. We use the following relation:

$$\mathbf{u}_n = N'v_c(\boldsymbol{\Omega} \times \mathbf{e}_m) - N_g(t_g)\mathbf{g}_n, \tag{84}$$

where N_g is considered as a function of time-to-go until intercept. We manipulate N_g in the simulation code to give some sense about its variation. The simulation results for $N' = 2, 3, 4, 5, 6$ and launch angles of $\gamma_L = 14, 20, 30, 40, 50, 60, 70$ deg are summarized in Table 1 using Eq. (84). The target with initial position of $[40\ 0\ 6]^T$ km flies at a velocity of $[-250\ 0\ 0]^T$ m/s. Therefore, the initial elevation angle of the target is 8.6 deg. The results show that an appropriate combination of g-bias and superelevation increase the final velocity. A small superelevation needs a larger g-bias.

Table 1. Simulation results for different vertical g-bias.

γ_L(deg)	N_g	N'	v_{m_f}(m/s)	t_f (s)
14	0	$3 \to 6$	$292 \to 368$	$47.4 \to 45.4$
	1	$2 \to 6$	$367 \to 416$	$45.3 \to 44.3$
	$N'/2$	$2 \to 6$	$367 \to 490$	$45.3 \to 42.9$
20	0	$3 \to 6$	$340 \to 394$	$45.7 \to 44.6$
	1	$2 \to 6$	$430 \to 438$	$43.8 \to 43.7$
	$N'/2$	$2 \to 6$	$430 \to 508$	$43.8 \to 42.4$
30	0	$3 \to 6$	$419 \to 431$	$43.7 \to 43.6$
	1	$2 \to 6$	$516 \to 471$	$42.1 \to 42.8$
	$N'/2$	$2 \to 6$	$516 \to 537$	$42.1 \to 41.8$
40	0	$2 \to 6$	$496 \to 463$	$42 \to 43$
	1	$2 \to 6$	$589 \to 501$	$41.3 \to 42.3$
	$N'/2$	$2 \to 6$	$589 \to 563$	$41.3 \to 41.5$
50	0	$2 \to 6$	$585 \to 493$	$41 \sim 42.5$
	1	$2 \to 6$	$653 \to 528$	$41.2 \sim 42$
	$N'/2$	$2 \to 6$	$653 \to 587$	$41.2 \sim 41.4$
60	0	$2 \to 6$	$661 \to 521$	$41.4 \sim 42.3$
	1	$2 \to 6$	$702 \to 554$	$41.4 \sim 42.4$
	$N'/2$	$2 \to 6$	$702 \to 609$	$41.5 \sim 42.4$
70	0	$2 \to 6$	$718 \to 548$	$42.1 \sim 43.4$
	1	$2 \to 6$	$720 \to 578$	$42 \sim 45.5$
	$N'/2$	$3 \to 6$	$707 \to 630$	$42 \sim 43$

We are now to choose a time-varying function for N' and N_g by trial and error to achieve a larger value for v_{m_f}. For example, for the mentioned target and $\gamma_L = 14$ deg, we obtain

$$N' = \begin{cases} 2 & \text{for } t_g \ge 30 \\ 5 - 0.1t_g & \text{for } 10 < t_g < 30 \\ 4 & \text{for } t_g \le 10 \end{cases} \tag{85}$$

$$N_g = \begin{cases} 6.5 & \text{for } t_g \ge 30 \\ 1 + 0.275(t_g - 10) & \text{for } 10 < t_g < 30 \\ 1 & \text{for } t_g \le 10 \end{cases} \tag{86}$$

which gives $v_{m_f} = 630.8$ m/s and $t_f = 44.84$ sec. The maximum value of final velocity in Table 1 for $\gamma_L = 14°$ is 490 m/s. This setting causes failure in the intercept for launch angles greater than 31.4°. For this launch angle ($\gamma_L = 31.4°$) we have $v_{m_f} = 434$ m/s and $t_f = 67.2$ sec.

For $\gamma_L = 70°$ and the mentioned target, $N_g = 0$ and N' is selected as

$$N' = \begin{cases} 1.5 & \text{for } t_g \geq 31 \\ 3 - \frac{1.5}{29}(t_g - 2) & \text{for } 2 < t_g < 31 \\ 3 & \text{for } t_g \leq 2 \end{cases} \quad (87)$$

which gives $v_{m_f} = 722$ m/s and $t_f = 45.14$ sec. The simulation results for smaller launch angles are given in Table 2. For smaller launch angles the final speed decreases up to $\gamma_L = 15°$. The interceptor misses its target for $\gamma_L \leq 15°$. We utilized the relation $t_g = r/v_c$ for Eqs. (85-87).

If the interceptor is fired at $\gamma_L = 34.33$ deg, it will intercept the target unguidedly at 539 m/s and 41.9 sec. In this case, $\Delta V = \int_0^{t_f} |u| dt = 0$ and $\int_0^{t_f} u^2 dt = 0$. It follows that midcourse guidance laws based on GCC can produce at most a final velocity of 539 m/s. Figure 1 shows the trajectories of three guidance laws and GCC, that is,

1. PN with $N' = 3.5$ ($N_g = 0$) and $\gamma_L = 30°$ labeled by PN in the figure,
2. PN with vertical g-bias of Eqs. (85,86) with launch angle $\gamma_L = 14°$ labeled by no. 2,
3. PN with variable N' of Eq. (87) with $\gamma_L = 70°$ labeled by no. 3,
4. and GCC, i.e., unguided trajectory ($\gamma_L = 34.33°$, $u_n = 0$).

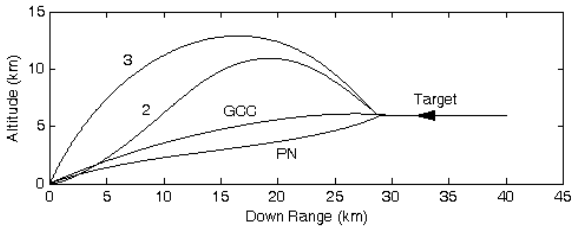

Figure 1. Comparison of four guidance trajectories.

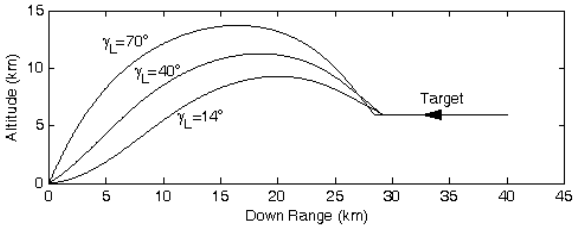

Figure 2. Modified guidance trajectories for different launch angles.

Table 2. Simulation results for different launch angles.

γ_L (deg)	v_{m_f} (m/s)	t_f (s)
≤ 15	No	Intercept
16	171	49.43
20	291	47.1
25	357	45.06
30	420	43.61
35	474	42.57
40	523	41.84
45	567	41.39
50	609	41.22
55	648	41.36
60	682	41.89
65	709	43.01
70	722	45.14

It is concluded that superelevation is more convenient than increasing vertical g-bias for surface-to-air applications. Air-to-air interceptors are usually fired with zero elevation angle, so a large vertical g-bias is needed at first to increase the flight-path angle for medium-to-long range missions. Equations (85-87) are obtained only for the mentioned initial conditions. In other words, these functions must be obtained in terms of target initial position and velocity for a specified launch angle. Therefore, a complicated function or an extensive look up table is needed for N', N_g, and γ_L.

To simulate modified midcourse guidance, Eq. (59) is utilized for estimating t_g with $\bar{v}_m = 900$ m/s. Also, Eq. (7) simplifies to

$$\mathbf{v}_{m_{cc}} = \left(\mathbf{r} + \mathbf{v}_t t_g - \frac{1}{2}\mathbf{g}t_g^2\right)/\beta_1(t_f, t). \quad (88)$$

Next, using an adjustment to Eq. (40) gives the following relation for γ_e (in deg):

$$\gamma_e(t) = 65\left(\frac{t_g^* - 8}{t + t_g^*}\right) \qquad \text{for } t_g^* > 8 \quad (89)$$

The commanded acceleration is given by

$$\mathbf{u}_n = 4(v_m/t_g^*)(\mathbf{e}_m \times \mathbf{e}_m^*) \times \mathbf{e}_m \qquad \text{for } t_g^* > 8 \quad (90)$$

and Eq. (84) with $N' = 4$ and $N_g = 0$ for $t_g^* \leq 8$.

The trajectories for this simplified guidance are shown in Figure 2 for $\gamma_L = 14, 40, 70°$. It is seen that even simplified relations for the proposed guidance due to limitation of computational burden, can work satisfactorily for different launch angles. Therefore, it can be utilized for both surface-to-air and air-to-air interceptors. A launcher with a fixed elevation angle can also be used for surface-to-air interceptors. The simulation results can be found in Table 3 for three different values of $\bar{v}_m = 800, 900, 1000$ m/s. It implies that the guidance law is not very sensitive to the value of $\bar{v}_m$, and γ_e has a dominant effect.

Table 3. Simulation results for simplified midcourse strategy at different values of γ_L and $\bar{v}_m$.

γ_L(deg)	$\bar{v}_m$(m/s)	v_{m_f}(m/s)	t_f (s)
14	800	626	43.80
	900	623	43.19
	1000	617	42.76
40	800	693	44.54
	900	693	43.49
	1000	688	42.77
70	800	711	48.43
	900	723	46.37
	1000	724	45.01

The relation for γ_e can be determined by numerical optimization in order to train a neural network or to develop an explicit relation. Training a neural network has been presented by Song and Tahk [7-9] for a surface-to-air interceptor. They proposed two guidance methods, namely, the γ-correction guidance law and the $\dot{\sigma}$-feedback guidance law (σ is the LOS angle). In their studies, flight path angle was trained using numerical optimization. The γ-correction guidance law do not work even for stationary targets, so they used a hybrid γ-correction + $\dot{\sigma}$-feedback guidance law to intercept stationary targets. In another work, they trained this hybrid guidance to intercept ballistic targets in minimum time [9], but atmospheric targets are intelligent, and change direction and altitude. Training a neural network using optimization data becomes more complicated for altitude constraints. In addition, training is needed for each type of interceptor. Training a neural network or fuzzy system for γ_e is more reasonable than the commanded acceleration or flight path angle especially for intelligent targets.

CONCLUSIONS

Analytical solution to an interceptor trajectory has been obtained considering drag and thrust forces in the presence of gravity. This formulation allows us to construct guidance laws based on GCC, which are near optimal for a considerable flight time toward the end, but modification is needed for the first stage of flight. The proposed conceptual strategy is a modification of midcourse strategies based on the GCC by increasing flight path angle with respect to GCC mainly for the first stage of flight. A new recursive relation for estimation of time-to-go for the GCC has been presented which reduces the onboard computational burden. Two other recursive relations for time-to-go have been obtained for optimal guidance laws. The relations can be used for both midcourse and terminal applications. The conceptual midcourse method is very flexible. It can cover various intercept geometries. A launcher with fixed elevation angle can also be used for surface-to-air interceptors.

The relation for γ_e can be determined by numerical optimization to develop an explicit relation. Also, training a neural network or fuzzy rules and membership functions for γ_e is more reasonable than the commanded acceleration or flight path angle especially for targets with different altitudes. Moreover, tactical issues can be considered in the midcourse guidance law more practically in the relation of γ_e.

Moreover, a combination of superelevation and vertical g-bias has been applied for two modified PN strategies. A little superelevation needs a larger g-bias. It has been concluded that superelevation is more convenient than increasing vertical g-bias for surface-to-air interceptors. In this case, effective navigation ratio in the vertical plane channel is chosen as time-varying which increases from small values (even smaller than 2) to its desired value for terminal guidance. Air-to-air interceptors are usually fired with zero elevation angle, so a large vertical g-bias is needed at first to increase the flight-path angle for medium to long range missions. The performance of PN strategies with vertical g-bias is highly dependent on the target position and velocity. Therefore, a complicated function or an extensive lookup table will be needed; otherwise, with target changing directions, inappropriate initial settings will cause intercept failure.

REFERENCES

1. Imado, F., Kuroda, T., and Miwa, S., "Optimal Midcourse Guidance for Medium-Range Air-to-Air Missiles", *Journal of Guidance, Control, and Dynamics*, **13**(4), PP 603-608(1990).
2. Kumar, R. R., Seywald, H., Cliff, E. M., and Kelley, H. J., "Three-Dimensional Air-to-Air Missile Trajectory Shaping", *Journal of Guidance, Control, and Dynamics*, **18**(3), PP 449-456(1995).
3. Cheng, V. H. L., and Gupta, N. K., "Advanced Midcourse for Air-to-Air Missiles", *Journal of Guidance, Control, and Dynamics*, **9**(1), PP 135-142(1986).
4. Menon, P. K. A., and Briggs, M. M., "Near-Optimal Midcourse Guidance for Air-to-Air Missiles", *Journal of Guidance, Control, and Dynamics*, **13**(4), PP 596-602(1990).
5. Katzir, S., Cliff, E., M., and Lutze, F. H., "An Approach to Near-Optimal Guidance On-Board Calculation", *IEEE ICCON*, (1989).
6. Kumar, R. R., Seywald, H., and Cliff, E. M., "Near-Optimal Three-Dimensional Air-to-Air Missile Guidance against Maneuvering Target", *Journal of Guidance, Control, and Dynamics*, **18**(3), PP 457-464(1995).
7. Song, E.-J., and Tahk, M.-J., "Real-Time Midcourse Guidance with Intercept Point Prediction", *Control Engineer Practice*, **6**, PP 957-967(1998).
8. Song, E.-J., and Tahk, M.-J., "Real-Time Midcourse Guidance Robust against Launch Conditions", *Control Engineer Practice*, **7**, PP 507-515(1999).

9. Song, E.-J., and Tahk, M.-J., "Real-Time Neural-Network Midcourse Guidance", *Control Engineer Practice*, **9**, PP 1145-1154(2001).

10. Raju, P. A., and Ghose, D., "Empirical Virtual Sliding Target Guidance Law Design: An Aerodynamic Approach", *IEEE Transactions on Aerospace and Electronic Systems*, **39**(4), (2003).

11. Jalali-Naini, S. H., and Pourtakdoust, S. H., "Modern Guidance Law in the Endoatmosphere", Proceedings of the 13th Iranian Conference on Electrical Engineering, Zanjan, Iran, PP 416-423(2005).

12. Jalali-Naini, S. H., and Pourtakdoust, S. H., "Modern Midcourse Guidance Law in the Endoatmosphere", *AIAA-2005-6291*, AIAA Navigation, Guidance, and Control Conference, San Francisco, CA, USA, (2005).

13. Riggs, T. L., "Linear Optimal Guidance for Short Range Air-to-Air Missiles", *IEEE 1979 National Aerospace Electronics*, PP 757-764(1979).

14. Lin, C.-F., *Modern Navigation, Guidance, and Control Processing*, Prentice-Hall, Englewood Cliffs, NJ, (1991).